Chapter 2:

Intracavity OptoGalvanic Spectroscopy not suitable for ambient level radiocarbon detection

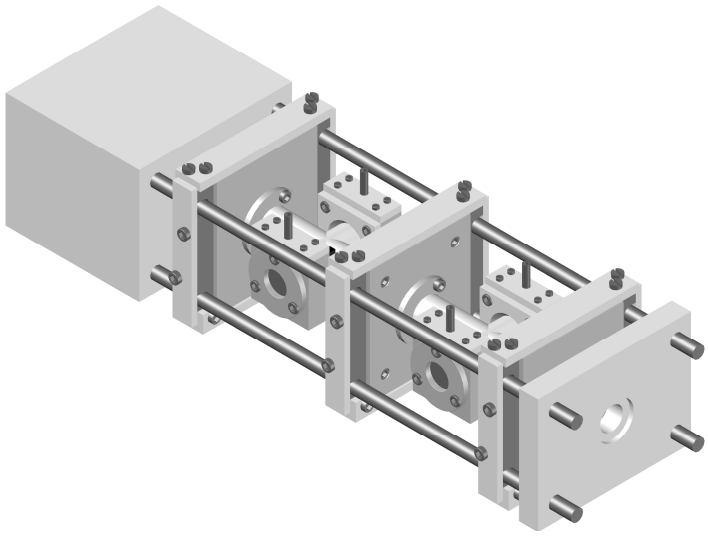

This chapter has been published as:

Paul, D.; Meijer, H. A. J., Analytical Chemistry 2015, 87, 9025-9032.

Cover image shows the intracavity cells placed inside the $^{14}CO_2$ laser gain medium for optogalvanic detection of radiocarbon described in this chapter.

Abstract

IntraCavity OptoGalvanic Spectroscopy (ICOGS) as a radiocarbon detection technique was first reported by the Murnick group at Rutgers University, Newark, USA in 2008. This technique for radiocarbon detection was presented with tremendous potentials for applications in various fields of research. Significantly cheaper, this technique was portrayed as a possible complementary technique to the more expensive and complex Accelerator Mass Spectrometry. Several groups around the world started developing this technique for various radiocarbon related applications. The ICOGS setup at the University of Groningen was constructed in 2012 in close collaboration with the Murnick group for exploring possible applications in the fields of radiocarbon dating and atmospheric monitoring. In this chapter we describe a systematic evaluation of the ICOGS setup at Groningen for radiocarbon detection. Since the ICOGS setup was strictly planned for dating and atmospheric monitoring purposes, all the initial experiments were performed with CO_2 samples containing contemporary levels and highly depleted levels of radiocarbon. Because of recurring failures in differentiating the two CO_2 samples, with radiocarbon concentration 3 orders of magnitude apart, CO_2 samples containing elevated levels of radiocarbon were prepared in-house and experimented with. All results obtained thus far at Groningen are in sharp contrast to the results published by the Murnick group and rather support the results put forward by the Salehpour group at Uppsala University. From our extensive test work, we must conclude that the method is unsuited for ambient level radiocarbon measurements, and even highly enriched CO_2 samples yield insignificant signal.

2.1 Introduction

In 2008, Murnick et al. (will be referred as “Mu2008” throughout this chapter), introduced ICOGS as a highly sensitive technique for radiocarbon (^{14}C) detection (Murnick et al. 2008). ICOGS evolved from its predecessor Laser Assisted Ratio Analyzer (LARA) which was developed and successfully used for $\delta^{13}C$ measurements for breath analysis (Murnick and Peer 1994; Murnick et al. 1995; Cave et al. 1999; Van der Hulst et al. 1999; Savarino et al. 2000) and in atmospheric CO_2 (Okil 2004). ICOGS was presented with tremendous potentials due to the underlined capabilities and did bring in hopes for an accelerator-free, thus affordable, laser-based radiocarbon detection method(Murnick and Okil 2005; Murnick et al. 2007; Murnick et al. 2008; Ilkmen 2009; Ilkmen and Murnick 2010; Murnick et al. 2010). The key features that made ICOGS attractive were: 1) minimal sample handling since samples were measured in the form of pure CO_2 or CO_2 mixed with a buffer gas such as N_2; 2) depending on the sample size measurements were possible in continuous flow-through and batch mode; 3) relatively simple and inexpensive construction when compared to an Accelerator Mass Spectrometer; and 4) projected detection limits close to or better than possible with AMS ($^{14}C/^{12}C \approx 10^{-15}$). With all these salient features, ICOGS could have potentially been useful in several fields of research, such as radiocarbon dating, industrial flue gas analysis, atmospheric monitoring, drug-metabolism studies, to name but a few.

ICOGS claimed its “allegedly” extraordinary sensitivity due to the combination of optogalvanic effect (OGE) and the intracavity enhancements achieved by the placement of sample cell inside the laser cavity. To reduce the interferences from the much more abundant molecular species e.g., $^{12}C^{16}O_2$, $^{13}C^{16}O_2$, $^{12}C^{18}O_2$, $^{13}C^{18}O_2$, $^{12}C^{17}O_2$, $^{13}C^{17}O_2$ etc., wavelengths around 11–12 µm were used. A commercially available CO_2 laser was modified to accommodate the sample cell inside the laser cavity. The CO_2 in the gas mixture, inside the laser gain medium, was replaced with $^{14}CO_2$ to generate the $^{14}CO_2$ specific wavelengths (11–12 µm) for higher specificity and sensitivity.

Following the 2008 publication, at least four groups around the world, including us at the University of Groningen got involved in the development of ICOGS for various applications. The ICOGS setup at Groningen was started in 2012, prior to which both authors spent a considerable time (DP ≈ 11 months, HAJM ≈ 3 months) in the Murnick group at Rutgers University, Newark. During the stay, we were involved in the day-to-day experiments conducted in the Murnick group, apart from understanding the technical details concerning the instrumentation. Experiments described in Mu2008 (Murnick et al. 2008) and elsewhere (Ilkmen 2009; Murnick et al. 2010) were repeated numerous times, using pure CO_2 and CO_2 mixed in different buffer gases (N_2 and Air), but none produced any reproducible results and conclusive evidence. Because of these severe reproducibility problems we encountered during the stay, it was extremely difficult to ascertain and conclude the feasibility of ICOGS. This led us to doubt the truthfulness of the previously published data and hence we decided to continue with the project in Groningen, with several modifications and careful evaluation criteria in mind.

Recently, the Salehpour group at Uppsala University have published their findings and reported their failure to reproduce the claim published in Mu2008 (Eilers et al. 2013; Persson et al. 2013; Persson and Salehpour 2015). The authors have extensively tested their ICOGS system in the ^{14}C concentration range of 29-970 percent of Modern Carbon (pMC) (Persson and Salehpour), so up to about tenfold the ^{14}C concentration in modern organic material. Several improvements in the excitation and detection methods were made but nevertheless, none of the experiments supported the claimed sensitivities of Mu2008 (Persson et al. 2014a; Persson et al. 2014b; Persson and Salehpour 2015).

Here we show results obtained using CO_2 samples for a very wide range of the $^{14}CO_2/^{12}CO_2$ ratio, from 10^{-15} to 10^{-3}. Initially all experiments were performed with CO_2 containing depleted levels of radiocarbon ($^{14}CO_2/^{12}CO_2 \leq 10^{-15}$) and CO_2 containing natural levels of radiocarbon ($^{14}CO_2/^{12}CO_2 \approx 10^{-12}$). Experiments were repeated numerous times, and under different conditions, but no obvious difference in OptoGalvanic Signal (OGS) from the two CO_2 samples was observed. Hence, CO_2 samples containing levels of radiocarbon elevated by many orders of

magnitude ($^{14}CO_2/^{12}CO_2 \approx 10^{-11}$ - 10^{-3}) were later prepared in-house to investigate the concentration range where a clear signal arising from radiocarbon could be detected.

2.2 Experimental setup

The ICOGS setup at Groningen (pictures shown in Figures 1 and 2 of Appendix II) is similar to the setup at Rutgers with some distinct modifications. As described in Mu2008 and elsewhere(Murnick et al. 2008; Ilkmen 2009), the setup at Rutgers consisted of a sealed reference cell positioned outside the laser cavity with highly elevated $^{14}CO_2$ concentration (1-10% $^{14}CO_2/^{12}CO_2$), and a sample cell that was placed inside the laser cavity. In contrast to the Rutgers setup, we placed both the sample and the reference cell inside the laser cavity. The reference cell was also a flow-through cell, identical to the sample cell, and was filled with contemporary reference CO_2 instead of enriched CO_2. The positioning of the reference cell inside the laser cavity was motivated by the principle of identical treatment of sample and reference materials, as is a common procedure for stable isotope measurements. This principle leads in general to higher measurement precision and reproducibility for relative measurement methods. In addition, it prevented the presence and use of extremely enriched $^{14}CO_2$ samples in the vicinity of our AMS ^{14}C dating facility.

The schematic of our ICOGS setup is shown in **Figure 1**. The setup consists of two isotopic CO_2 lasers; a $^{12}CO_2$ laser (Merit-SZ, Access Laser Co., USA) and a customized $^{14}CO_2$ laser (Lasy-20GZ, Access Laser Co., USA) with emission lines between 10.532-10.741 μm and 11.258-11.891 μm, respectively. A list of all the laser lines emitted by the $^{14}CO_2$ laser is shown in **Table 1** (Freed 1995). With help from the manufacturer, the output coupler (1%) mounting block (OCMB in Figure 1) of the $^{14}CO_2$ laser was moved away from the gain medium, such that both the cells could be accommodated inside the extended cavity. The cells have a cross-shaped geometry (64 mm × 38 mm, OD = 15 mm, wall thickness = 2 mm) and are constructed from fused silica. For a clearer picture, one representative cell is shown in the inset of Figure 1 with a blue background. Two copper tapes (5 mm wide) are placed 25 mm apart along the long axis and are connected to the RF

excitation and detection electronics through coaxial cables. The RF excitation and detection electronics were based on the design of May et al. (May and May 1986). They were obtained from the Murnick Group, and are similar to the ones used at Rutgers. Using a custom built cell-mount, the two cells are precisely positioned inside the laser cavity. The ZnSe (II-VI Incorporated) windows along the $^{14}CO_2$ laser axis are connected to the cell through the cell mount. Additional mounts with the sample inlet/exit ports were used to connect the ZnSe windows to the transverse arms of the cells through which the $^{12}CO_2$ laser beam was directed into the two cells. The ZnSe windows were mounted parallel to each other, and no significant power loss was observed, so a Brewster angled window as in the Rutgers setup was deemed unnecessary. Two power meters (30A-BB-18 for the $^{12}CO_2$ laser and 3A for the $^{14}CO_2$ laser, Ophir Photonics) were installed to continuously monitor the laser power. A spectrum analyzer (16E-C14, Macken Instruments Inc., USA) was used to verify the laser wavelength whenever the $^{14}CO_2$ laser was tuned to a desired wavelength. Since it was extremely difficult to spot the laser beam on the spectrum analyzer's infrared sensitive phosphor screen when the laser power was below 70 mW, an infrared camera (FLIR, i7) was often used to detect the diffracted beam on the screen. Gold-coated mirrors (Part number 43-733, Edmund Optics) were used to steer the beam through the cells to the power meters. Two mass flow controllers (πMFC-LP P2A, MKS) were used to introduce CO_2 into each cell and two pressure controllers (Model-640B, MKS) were used upstream to regulate the cell pressure. The flow rates and pressures explored were in the range of 0.2-0.5 sccm (standard cubic centimeters per minute) and 100-1200 Pa, respectively.

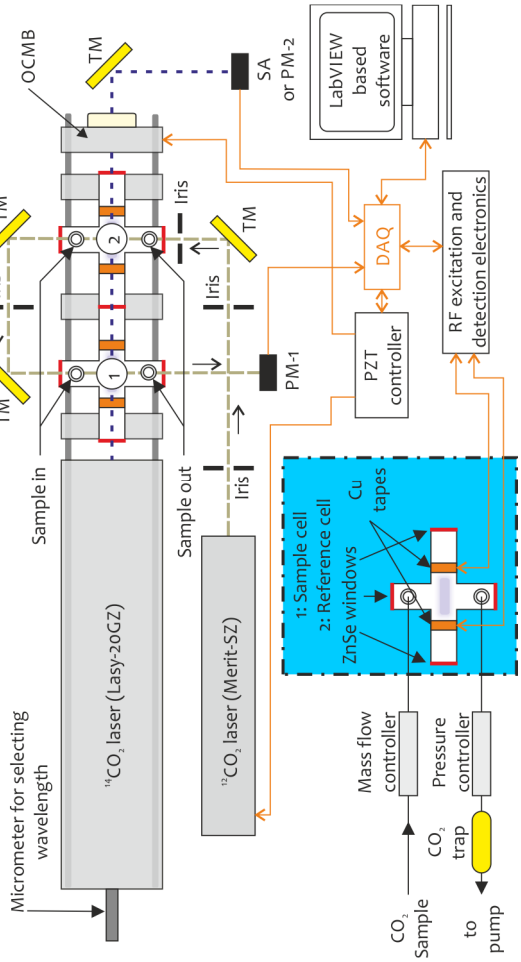

Figure 1: Schematic diagram showing the ICOGS setup at the University of Groningen. The setup consists of two isotopic CO_2 lasers, two sample cells, beam steering optics, a spectrum analyzer and two power meters. The sample and reference cell are both located inside the $^{14}CO_2$ laser cavity. The two copper electrodes are placed 2.5 cm apart (shown in the inset with blue background) and are connected to the RF excitation and detection electronics. The other components indicated with abbreviations are as follows: TM Turning Mirror; OCMB Output Coupler Mounting Block; PM Power Meter; SA Spectrum Analyzer; PZT Piezoelectric Transducer; DAQ Data Acquisition and Control; RF Radio Frequency. The laser beams are shown with dashed lines and the data handling with solid lines.

Line	Wavenumber (cm^{-1})	Wavelength (μm)	Frequency (MHz)
P(30)	841.00066805	11.8906	25212565.7454
P(28)	842.78929784	11.8654	25266187.5176
P(26)	844.56171722	11.8405	25319323.3138
P(24)	846.31793897	11.8159	25371973.5173
P(22)	848.05797276	11.7916	25424138.4180
P(20)	849.78182521	11.7677	25475818.2143
P(18)	851.48949996	11.7441	25527013.0154
P(16)	853.18099777	11.7208	25577722.8440
P(14)	854.85631653	11.6979	25627947.6369
P(12)	856.51545136	11.6752	25677687.2478
P(10)	858.15839460	11.6529	25726941.4470
P(8)	859.78513592	11.6308	25775709.9249
R(8)	872.95574563	11.4553	26170554.8708
R(10)	874.42754754	11.4361	26214678.3820
R(12)	875.88287985	11.4171	26258308.1470
R(14)	877.32170194	11.3983	26301442.9481
R(16)	878.74397043	11.3799	26344081.4848
R(18)	880.14963923	11.3617	26386222.3753
R(20)	881.53865943	11.3438	26427864.1533
R(22)	882.91097929	11.3262	26469005.2677
R(24)	884.26654418	11.3088	26509644.0807
R(26)	885.60529650	11.2917	26549778.8656
R(28)	886.92717564	11.2749	26589407.8052
R(30)	888.23211790	11.2583	26628528.9900

Table 1: List of all the laser lines emitted by the $^{14}CO_2$ laser (LASY-20GZ)[18]. Optogalvanic response of CO_2 containing depleted levels of ^{14}C and CO_2 containing natural levels of ^{14}C were evaluated at all lines the laser emitted. More extensive experiments were performed between P(20) and P(28).

2.3 Samples used

Based on our experience with the ICOGS setup at Rutgers, we were more inclined towards testing our ICOGS setup with pure CO_2. This was mostly because of the severe reproducibility issues we faced at Rutgers with the CO_2-in-N_2 based system in almost all experimental conditions we worked with, and also that the pure CO_2

based system was relatively less explored. Taking advantage of the in-house AMS facility at Groningen, we could use several well-characterized AMS local reference gases, in the whole natural range. To establish the optimal experimental conditions required for the best signal discrimination, we worked with a CO_2 gas highly depleted in ^{14}C ($^{14}C/^{12}C$ < 0.1 pMC), called "dead" from now on, and a CO_2 gas with a contemporary ^{14}C concentration ($^{14}C/^{12}C$ ≈ 108.8 pMC), called "modern" from now on. According to the claims from Mu2008 it should have been easy to see clear differences in the optogalvanic response at the P(20) transition (11.7677 μm) from the two gases with ^{14}C concentrations ≈3 orders of magnitude apart. Over a period of more than a year, many attempts were made to reproduce the claims, but none yielded evidence of unambiguous radiocarbon detection. During the same period, Persson et al. (Persson et al. 2013), also published their findings and questioned the validity of ICOGS, which also supported our findings. We then suspected that the actual detection limit achievable was much above the claimed detection limits. Hence, we decided to prepare a series of CO_2 local reference gases containing elevated levels of $^{14}CO_2$. A 0.5% $^{14}CO_2/CO_2$ sample was ordered from ViTrax Radiochemicals, USA to prepare these local reference gases (listed in **Table 2**). The 0.5% $^{14}CO_2/CO_2$ was diluted in steps with dead CO_2 to prepare a series of nine local reference gases ($^{14}CO_2/CO_2 \approx 10^{-3}$ to 10^{-11}) with very similar $\delta^{13}C$ values. To avoid any additional contribution to the OGS arising from the variations in the ^{13}C concentration, we diluted the nine samples with a single gas, the dead CO_2. To ensure the correctness of this dilution procedure, the last sample in the series containing the lowest amount of radiocarbon, namely one order of magnitude higher than contemporary based on the dilution scheme, was analyzed at the Groningen AMS facility. For obvious reasons of contamination in the AMS facility, other samples in the series containing 100 - 1 billion times contemporary radiocarbon concentrations were not measured. The activities of these enriched samples were then calculated, based on knowledge of the dilution ratio and the activity of the last sample, as determined by the AMS measurement. The AMS measurement of the last sample yielded $^{14}C/^{12}C \approx 9.5\times10^{-12}$ (or a normalized activity of 951.1 ± 2.3 % to be exact), which matched the targeted value within the concentration uncertainty of the original 0.5% sample, thereby demonstrating the

correctness of our dilution process (the results imply that the 0.5% $^{14}CO_2/CO_2$ sample in fact had a $^{14}CO_2/CO_2$ ratio of 0.47%). The $\delta^{13}C$ value of the original $^{14}CO_2$ gas is unknown, but according to the supplier it is in the natural range. This means that due to the high level of dilution of the samples, the $\delta^{13}C$ value for all except perhaps the first are virtual identical to that of the dilution gas.

Sample	Intended ($^{14}CO_2/^{12}CO_2$)	Calculated ($^{14}CO_2/^{12}CO_2$)
1	1.01×10^{-3}	9.57×10^{-4}
2	1.01×10^{-4}	9.56×10^{-5}
3	1.01×10^{-5}	9.57×10^{-6}
4	1.01×10^{-6}	9.55×10^{-7}
5	1.01×10^{-7}	9.52×10^{-8}
6	1.01×10^{-8}	9.54×10^{-9}
7	1.01×10^{-9}	9.55×10^{-10}
8	1.01×10^{-10}	9.53×10^{-11}
9	1.01×10^{-11}	**9.50×10^{-12} ***

Table 2: Summary of the samples enriched in radiocarbon prepared by diluting commercially available 0.5% $^{14}CO_2/CO_2$ with CO_2 highly depleted in radiocarbon. The $^{14}C/^{12}C$ value for the last sample in the series was determined by AMS measurement at Groningen (indicated by *). The $\delta^{13}C$ value for all except perhaps the first (see text) are virtually identical to that of the dilution gas, which has a $\delta^{13}C$ value of -3.4 ‰.

2.4 Results and discussions

As mentioned earlier, ICOGS for radiocarbon detection was presented with several attractive features, one of the most appealing being the ability to perform measurements on pure CO_2 in both flow and batch mode, depending on the sample size. To optimize the experimental parameters of ICOGS, all the initial experiments were performed with both dead and modern CO_2 in a continuous flow mode. Since unambiguous detection of radiocarbon in the range of dead to modern, with a pure CO_2 based system, was not achieved even after many attempts, we decided to reexamine the claimed detection limits. This was only possible if several CO_2 samples containing different and elevated concentrations of $^{14}CO_2$ would be introduced and the change in optogalvanic signal as a function of

concentration derived. Hence, as described in the earlier section, nine enriched CO_2 samples were prepared in-house to investigate the achievable detection limits. These experiments with elevated radiocarbon concentration were performed only in batch mode because of reasons described later.

2.4.1 Continuous-flow mode measurement

Several different reactions take place inside a CO_2 glow discharge(Williams and Smith 2000; Okil 2004; Spencer and Gallimore 2010), the most important being the dissociation of CO_2 to CO. Since different gases influence the optogalvanic response of the analyte gas in different ways, by affecting the rate of ionization, it is very important to have a consistent gas mixture. Continuous-flow mode measurements ensure that the gas inside the discharge is always refreshed and thus one would avoid the accumulation of dissociated product that may influence the optogalvanic response in undesirable ways. Hence flow mode experiments became the very obvious choice to probe the ^{14}C detection capabilities of ICOGS. A multitude of different pressure and flow ranges were examined to document the optogalvanic response and the corresponding signal-to-noise ratio. The OptoGalvanic Signal (OGS) for both the dead and modern CO_2 was investigated at almost all $^{14}CO_2$ laser emission lines mentioned in **Table 1** which includes R(8)-R(30) and P(10)-P(30). The largest OGS was always achieved at the resonant P(20) transition and this transition was also used extensively by the Murnick group(Murnick et al. 2008; Ilkmen 2009), hence this transition was used with the continuous flow through experiments. A typical example of those many experiments performed to see the optogalvanic response of CO_2 with different radiocarbon concentration is shown in **Figure 2**. During this experiment, pure CO_2 was continuously flushed through the system at a flow rate of 0.2 sccm with a pressure of 800 Pa. The $^{14}CO_2$ and the $^{12}CO_2$ lasers were electronically chopped at a frequency of 131 Hz and 97 Hz respectively. By applying a Fast Fourier Transformation (FFT) to the resultant optogalvanic waveform obtained from each cell, the signal amplitudes at the two fundamental chopping frequencies are calculated. These amplitude signals from the sample and reference cells

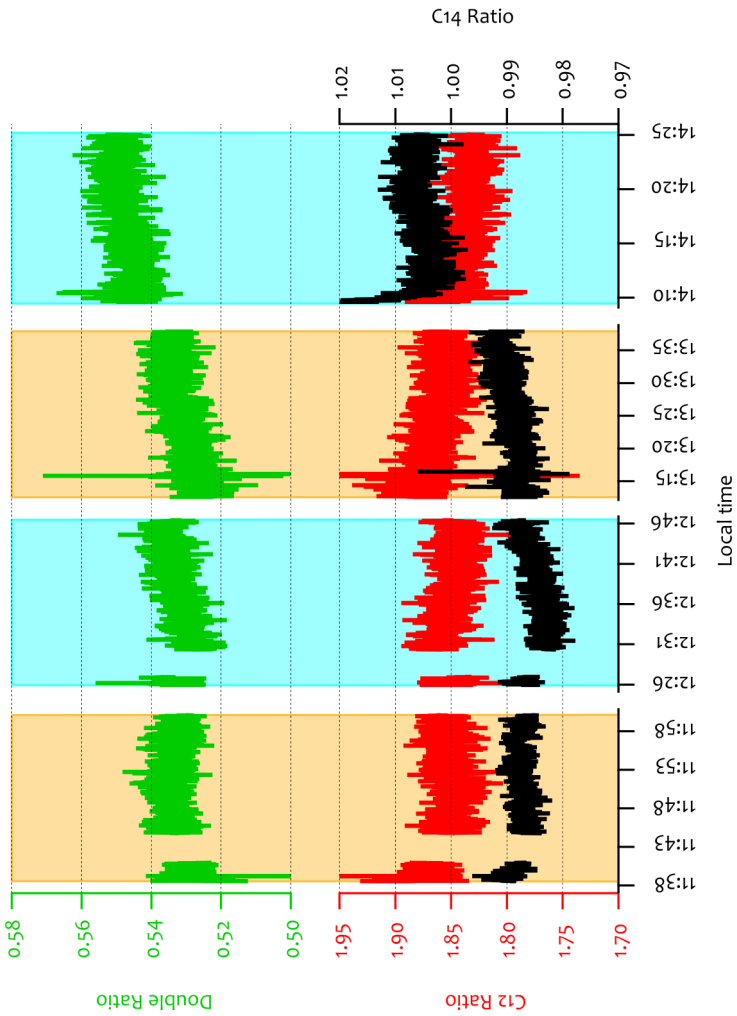

Figure 2: A data set showing continuous measurement of CO_2 through the reference and the sample cell. The C12 and the C14 ratios, shown in the lower part of the figure, are represented by the red line and black line, respectively. The green line shows the corresponding double ratio in the upper half of the figure. The orange background indicates the ratios when identical gas, dead CO_2, was introduced in both cells. Indicated with blue backgrounds are the ratios when different gases, dead CO_2 in the reference cell and modern CO_2 in the sample cell, were introduced. No significant difference in the double ratio is observed.

corresponding to the $^{14}CO_2$ and $^{12}CO_2$ laser chopping are called $^{14}C_{Sam}$,$^{14}C_{ref}$ and $^{12}C_{Sam}$,$^{12}C_{ref}$ respectively. At 800 Pa, the OGS produced by the $^{14}CO_2$ laser chopping at the P(20) transition was more than 3 times higher than at 130 Pa, while the OGS produced by the $^{12}CO_2$ laser chopping was reduced by a factor of 2. As described in Mu2008 and elsewhere(Ilkmen 2009), the fluctuations arising from the laser can be eliminated by dividing the sample signal with the corresponding reference signal, producing the single ratios (C14 ratio = $^{14}C_{Sam}$ /$^{14}C_{ref}$; C12 ratio = $^{12}C_{Sam}$ /$^{12}C_{ref}$). To eliminate the discharge fluctuations, the two single ratios were then used to calculate the double ratio (i.e. ratio of ratios) [$^{14}C_{Sam}$ /$^{14}C_{ref}$]/[$^{12}C_{Sam}$ /$^{12}C_{ref}$], which is equivalent to [$^{14}C_{Sam}$ /$^{12}C_{Sam}$]/[$^{14}C_{ref}$ /$^{12}C_{ref}$]. This latter expression is identical to the double ratios that are commonly used in stable isotope analysis, and from which delta values are derived. In **Figure 2**, the C12 ratio (red line) and the C14 ratio (black line) are shown in the lower half of the plot. The corresponding double ratio (green line) is shown in the upper half of the plot. First, the reference and the sample cells were both filled with dead CO_2, shown with yellow background. The dead CO_2 from the sample cell was then evacuated and replaced with the modern CO_2, shown with blue background. This switching of the gas in the sample cell, while keeping the same gas in the reference cell, was performed multiple times. Differences in the optogalvanic response of gases containing varying concentrations of radiocarbon should have been clearly visible in this example, had the corresponding OGS been noticeably different. Through a series of similar experiments, with varying parameters e.g., pressure, flow, $^{14}CO_2$ laser chopping frequency etc., we noted again and again that our instrument was not capable of unambiguously differentiating modern from dead CO_2. On the other hand, we learned that small changes in pressure and flow had notable influence in the resultant signal, which could be misinterpreted as $^{14}CO_2$ signal if a careful evaluation and continuous monitoring of all parameters was not performed.

2.4.2 Batch mode measurement

From flow mode experiments described in the previous section it was clear that our instrument could not differentiate modern from dead CO_2. This made us believe

that the $^{14}CO_2$ sensitivity, based on the assumption of a degree of enhancement because of intracavity operation of ≈ 10^7, as in the case of Mu2008, was possibly not true with our system (or in fact not at all). It must be emphasized that, based on our experience with the ICOGS system described in Mu2008, an enhancement factor of ≈ 10^7, leading to high sensitivity, may be an exaggeration. Therefore we decided to carefully determine the true sensitivity of our ICOGS setup through experiments with CO_2 samples enriched in ^{14}C. Since CO_2 gases containing elevated levels (10^1 – 10^9 × natural abundance) of ^{14}C concentrations are unavailable commercially, we prepared these desired local reference gases with elevated levels of radiocarbon in-house. As a precautionary measure because of the possibility of ^{14}C contamination in the AMS facility, samples were prepared in an isotope laboratory located in a different building, a few hundred meters away from the AMS facility. For the same reason, the ICOGS laboratory, where the samples were used and stored after preparation, is also located far away from the AMS laboratory (albeit in the same building complex). Because of both the strict European regulation on release of radioactive material and limited sample size, the experiments with these samples were performed in batch mode. In contrast to the continuous flow measurements, the batch mode experiments were performed with only one cell. A one-cell measurement was preferred since it was practically impossible to identically tune the two discharges in batch mode. This would lead to a difference in the rate of dissociation of CO_2, indicated by difference in the rate of change of pressure in the cell. Since the OGS from the C-12 and the C-14 channels are non-linearly dependent on pressure, it would make the correction to the single and hence the double ratio complicated and error-prone. Therefore, to keep the analysis simple, we chose to use only one cell as it would allow us to investigate the initial levels of detection.

To prevent the enriched CO_2 from escaping into the laboratory, a trap containing Carbo-Sorb® was placed between the pressure controller and the vacuum pump. The Carbo-Sorb® adsorbent was later disposed according to the University of Groningen's radiochemical disposal procedure. Experimental conditions, between experiments, were kept as similar as possible in order to have a realistic

comparison. An example experiment showing the optogalvanic response of a CO_2 discharge, performed with Sample No. 1 ($^{14}C/^{12}C$ 9.57×10^{-4}, refer Table 1), at five different laser transitions is presented in **Figure 3**. CO_2 is introduced into the cell to a pressure of about 400 Pa. Once the pressure in the cell stabilized, the discharge was turned ON, which is characterized by a sharp, but small, rise in pressure. The laser was then tuned to a desired wavelength and allowed to stabilize, shown in white background. The length of the laser cavity was detuned by scanning a PZT placed on the output coupler. The selected voltage range (0-500 V) reveals one longitudinal mode, shown by a peak observed in the laser power, marked with gray background. The laser power was then stabilized on the maximum of the OGS, marked with yellow background. The DC offset associated with the discharge was determined by blocking the $^{14}CO_2$ laser, shown with orange background and is ≈ 0.4 mV in our case. To reduce the risk of contamination arising because of memory effects, the cell was evacuated for at least an hour before it was discharge cleaned with helium, shown with the pink background. This extra step of discharge cleaning was included in the cleaning procedure to remove the residual CO_2 from the glass surface (suggested by Prof. Daniel Murnick through personal communication), although the effectiveness was not verified. Following the helium discharge-cleaning step, the cell was evacuated again. This cleaning procedure was repeated every time before a new sample was introduced into the cell.

The objective with these one-cell experiments was to look for differences in the power normalized OGS as a function of the changing ^{14}C concentration in samples, and to do so at different laser transitions. OGS for the dead, modern and enriched CO_2 samples were measured in batch mode at the P(18)-P(30) range of $^{14}CO_2$ laser transitions listed in **Table 1**. The most extensive studies were performed between P(20)-P(28), such as illustrated in **Figure 3**. The most striking feature seen in **Figure 3** is the large OGS produced at the P(20) transition, which is not evident on any other laser transition we experimented with (mind the logarithmic vertical OGS axis in Figure 3). Unlike the other laser transitions, the peak optogalvanic signal at the P(20) transition is not located on the peak laser power, but on its shoulder. This feature indicated a possible coincidental resonance with

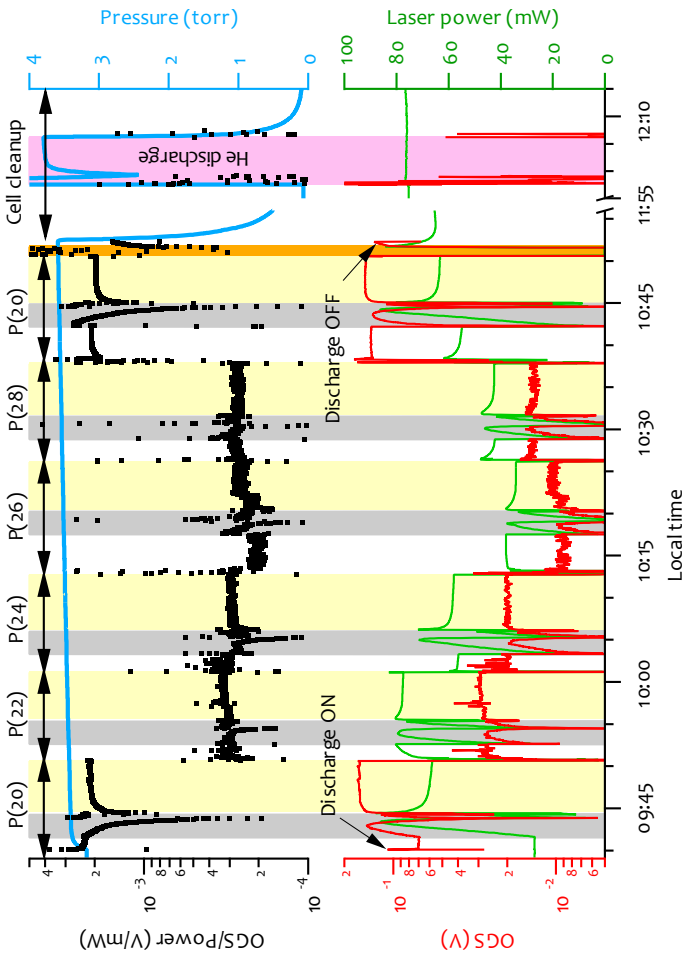

Figure 3: Experiment, performed in batch mode, showing the OGS of a pure CO_2 ($^{14}C/^{12}C \approx 0.1\%$) discharge at various $^{14}CO_2$ laser lines. A PZT scan to stabilize the OGS at the maximum, shown with gray background, is performed selecting the desired laser line. The laser is allowed to stabilize on the peak of the OGS for some time, shown with yellow background, before switching to, and stabilizing on, the next $^{14}CO_2$ laser line (white background). The OGS and the laser power are shown in the lower half of the graph. The power normalized OGS and the cell pressure are shown in the upper half of the graph. To reduce the memory effect, the cell is first evacuated, then discharge cleaned with helium, shown in pink background, and evacuated again before performing the next measurement. The DC offset on the OGS is determined by blocking the laser, shown with the orange background.

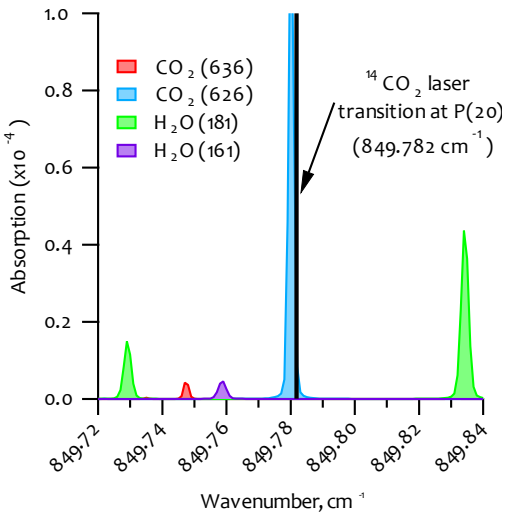

Figure 4: Simulation performed using HITRAN on the web (http://hitran.iao.ru/) to show the possible source of the enhanced OGS at the P(20) laser transition. An energetically high $^{12}C^{16}O_2$ transition is probably responsible for the large signal enhancements as seen in Figure 3. For the purpose of verification other molecules like $^{13}C^{16}O_2$, $H_2{}^{16}O$, and $H_2{}^{18}O$ have also been shown. For the different isotopologues, Air Force Geophysics Laboratory (AFGL) shorthand notations have been used (e.g., $^{16}O^{12}C^{16}O$ is represented as 626).

another, more abundant, interfering species in the discharge. From previous studies in the Murnick Group (Okil 2004), influence of water vapor leading to OGS enhancement was already known. It was thus predicted that water vapor contamination in the CO_2 samples might be the cause of the P(20) signal enhancement. We did a few tests to check the extent of signal enhancement by humidifying the samples. Results indicated that water vapor contamination in our system quenched the OGS instead of enhancing it. HITRAN simulations (performed at http://hitran.iao.ru/) then revealed the presence of an energetically high lying $^{12}C^{16}O_2$ transition ≈51 MHz from the P(20) laser transition, shown in **Figure 4**. It seems quite likely that this $^{12}C^{16}O_2$ transition accounts for the large intracavity OGS enhancement on the P(20) laser transition. This corruption of the OGS makes the P(20) transition unsuited for $^{14}CO_2$ detection in pure CO_2.

A summary of all the measurements made with six enriched working standards and the dead CO_2 are shown in **Figure 5a**. Every sample, shown in Figure 5a, was measured three consecutive times in the order of their increasing activity. The OGS corresponding to each sample is an average of the three measurements, and the error bars indicate 1σ standard deviation. The results indicate that there is no clear dependence of the OGS amplitude on the radiocarbon concentration. A few initial measurements with the highly ^{14}C enriched samples did, however, produce a noticeably higher OGS amplitude in the 10^{-4}-10^{-3} $^{14}C/^{12}C$ range. Similar to the detection sensitivities achieved by LARA, OGS at these ranges would be more realistic if there is no intracavity enhancement as claimed in Mu2008. Unfortunately, these results were not reproduced in the later set of measurements that contributed to Figure 5a. For all transitions (leaving the P(20) aside) the average OGS for dead CO_2 is higher than for all higher ^{14}C level gases. However, for three out of four transitions this is no significant effect: the large error bars for P(22) and P(24) are the result of considerable scatter of the individual measurements. Furthermore, from extensive tests described above, we know that there is no significant OGS difference between the dead and modern (10^{-12}) levels. Figure 5b shows an example of six independent batch mode measurements performed with the dead (D) and modern (M) CO_2 (3 each) at different laser lines. This example demonstrates the large variability in the OGS that frequently leads to substantial spread. It also shows that the difference in the OGS of dead and 10 × modern sample (10^{-11}), shown in Figure 5a, is not real and that the signals are all within the variability of the OGS. This large variability in the OGS leading to unsuccessful discrimination of OGS produced by CO_2 containing different levels of ^{14}C was also demonstrated by Persson et al., at Uppsala University (Persson et al. 2013). With this extra information, it is clear that these higher points at the lowest ^{14}C level are coincidental.

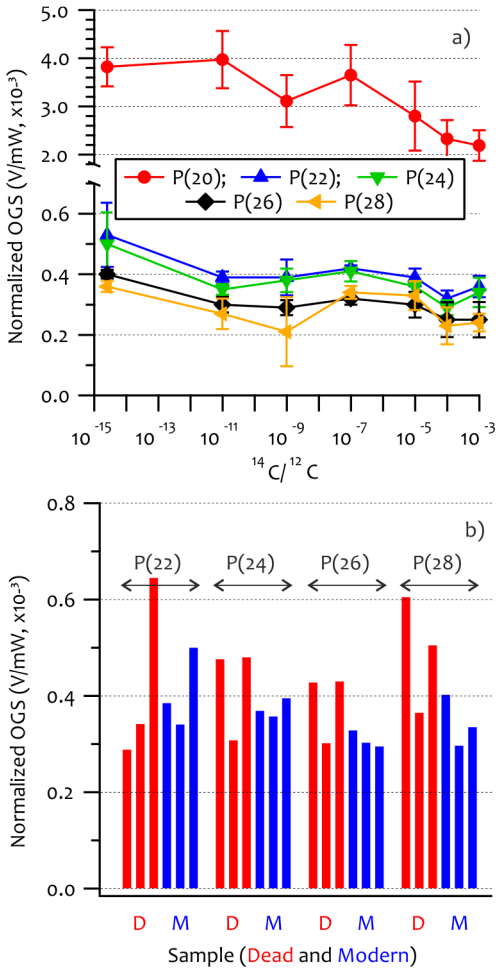

Figure 5: a) Summary of a series of twenty-one experiments performed with dead CO_2 and six enriched CO_2 samples in the sequence of their increasing activity. Each sample was measured three consecutive times; one such experiment is shown in Figure 4. The vertical error bars indicate 1σ standard deviation. No evidence showing dependence of the amplitude of OGS to the radiocarbon concentration was observed. **b)** Results showing OGS of a set of six independent batch-mode measurements of dead and modern CO_2 demonstrating the large variability in the OGS. These results demonstrate that the apparent difference in the dead and 10 × modern CO_2 OGS at P(22)–P(28), shown in a), are insignificant as they are within the detection variability.

2.5 Conclusions

Motivated by the claimed potentials of ICOGS described in Mu2008, at least four other research groups, including the University of Groningen, participated in developing ICOGS for various applications in collaboration with Rutgers. The construction of the ICOGS setup at Groningen was completed by mid-2012. Since then, extensive work has been done and a range of experimental strategies was employed with the goal to unambiguously detect radiocarbon signal in pure CO_2 samples. Because of repeated failures in the dead to modern range, we decided to also explore the range beyond the natural one, with CO_2 containing several-to-many orders of magnitude higher concentrations of radiocarbon, even though this concentration range was well beyond our area of interest. Even with these enriched CO_2 samples, we could not detect a clear OGS dependency on the radiocarbon concentration. Moreover, reproducing discharge conditions, which is another key parameter, was difficult and introduces the large variability observed in the signal. This problem of reproducibility, probably leading to false positive signal in the data presented in Mu2008 was suggested by the Uppsala group(Persson et al. 2013). From our extensive and detailed studies, we conclude that the level of detection is at the 10^{-3} level, to 10^{-4} at best. Further optimization would of course probably be feasible, but as the technique with even 10^{-5} level of detection would still be useless for our, and probably all, intended applications, we decided not to invest further time and resources.

From the results presented in the previous sections, we could not demonstrate ICOGS as a viable radiocarbon detection technique. Instead, through all our efforts as well as those of the group at Uppsala we have come as close as possible to proving that ICOGS is unsuited as a viable radiocarbon technique. Similar, unsuccessful results were also obtained at the Columbia University (through personal communications with Dr. Cantwell G. Carson). Even though there are some distinct differences in the setup, the RF excitation/detection electronics and our measurement/analysis scheme are very similar to the ones used by the Murnick group. Through our extensive experiments, we are very sure that the

results presented in Mu2008 are highly suspicious and for the purpose of scientific integrity must be withdrawn.

Of course, Optogalvanic Spectroscopy is a viable and proven trace gas detection technique. The LARA (Murnick and Peer 1994; Minoli et al. 1998; Cave et al. 1999; Van der Hulst et al. 1999; Savarino et al. 2000; Braden et al. 2001; Okil 2004; Murnick and Okil 2005) instrument is capable of measuring $^{13}CO_2/^{12}CO_2$ ratios in exhaled breath at a precision and accuracy level that makes it useful in clinical breath analysis applications. Based on that, we can estimate the level of detection of this, optimized flow-through system as $\geq 10^{-5}$, loosely based on a 10^{-3} (equivalent to 1 ‰ in $\delta^{13}C$ (Murnick and Okil 2005)) precision in detecting the 1.1% level of $^{13}CO_2$. The precision in the detection of a substantial signal is usually higher than the level of detection of a rare species, as in the former case signal averaging is used. For a fully optimized IntraCavity Optogalvanic System, the detection limit may even be better still, thanks to the higher intracavity laser power ($\approx \times 100$). This, however, would only be feasible by using a flow-through system of CO_2 in Nitrogen, as this dilution in Nitrogen gas is known to enhance the OGS considerably (Okil 2004). Measurement of such a mixture, however, introduces additional uncertainty effects. Because of the complex nature of optogalvanic spectroscopy and poor understanding of the magnitude of OGS generation at different wavelength, it becomes very difficult to ascertain the limit of detection as is possible in the case of absorption spectroscopy. The batch-mode measurements using a single cell, and pure CO_2 do definitely have a worse level of detection, such that the 10^{-3} or 10^{-4} level we cautiously report above are quite realistic. The alleged intracavity enhancement term introduced in Mu2008 has not been proven so far, and has not been underpinned theoretically either. In this work, we have come as closely as possible to proving that the results claimed in Mu2008 are incorrect. Thus, AMS is still the best possible method for high-precision ^{14}C measurements at subcontemporary levels, especially for age determination (“dating”). However, several laser based spectroscopic methods for radiocarbon detection have recently been demonstrated (McCartt et al. ; Galli et al. 2011; Galli et al. 2013; Genoud et al. 2015). Although some of these methods realize ^{14}C detection limits below 10^{-13},

currently none of them can compete with AMS in that respect. Most of the methods are more suitable and, in fact, designed for pharmaceutical and other applications that make use of ^{14}C labeling.

2.6 References

Braden B, Gelbmann C, Dietrich CF, Caspary WF, Scholmerich J, Lock G. 2001. Qualitative and quantitative clinical evaluation of the laser-assisted ratio analyser for detection of Helicobacter pylori infection by C-13-urea breath tests. European Journal of Gastroenterology & Hepatology 13(7):807-10.

Cave DR, Veldhuyzen van Zanten S, Carter E, Halpern EF, Klein S, Prather C, Stolte M, Laine L. 1999. A multicentre evaluation of the laser assisted ratio analyser (LARA): a novel device for measurement of $^{13}CO_2$ in the ^{13}C-urea breath test for the detection of Helicobacter pylori infection. Alimentary Pharmacology & Therapeutics 13(6):747-52.

Eilers G, Persson A, Gustavsson C, Ryderfors L, Mukhtar E, Possnert G, Salehpour M. 2013. The Radiocarbon Intracavity Optogalvanic Spectroscopy Setup at Uppsala. Radiocarbon 55(3–4):237-50.

Freed C. 1995. 4 - CO_2 Isotope Lasers and Their Applications in Tunable Laser Spectroscopy. In: Duarte FJ, editor. Tunable Lasers Handbook. San Diego: Academic Press. p 63-165.

Galli I, Bartalini S, Borri S, Cancio P, Mazzotti D, De Natale P, Giusfredi G. 2011. Molecular Gas Sensing Below Parts Per Trillion: Radiocarbon-Dioxide Optical Detection. Physical Review Letters 107(27):270802.

Galli I, Bartalini S, Cancio P, De Natale P, Mazzotti D, Giusfredi G, Fedi ME, Mando PA. 2013. Optical detection of radiocarbon dioxide: First results and AMS intercomparison. Radiocarbon 55(2-3):213-23.

Genoud G, Vainio M, Phillips H, Dean J, Merimaa M. 2015. Radiocarbon dioxide detection based on cavity ring-down spectroscopy and a quantum cascade laser. Optics Letters 40(7):1342-5.

Ilkmen E. 2009. Intracavity Optogalvanic Spectroscopy for Radiocarbon Analysis with Attomole Sensitivity [Doctoral Thesis]. Newark: Rutgers, The State University of New Jersey.

Ilkmen E, Murnick DE. 2010. High sensitivity laboratory based C-14 analysis for drug discovery. Journal of Labelled Compounds & Radiopharmaceuticals 53(5-6):304-7.

May RD, May PH. 1986. Solid-state radio frequency oscillator for optogalvanic spectroscopy: Detection of nitric oxide using the 2-0 overtone transition. Review of Scientific Instruments 57(9):2242.

McCartt AD, Ognibene T, Bench G, Turteltaub K. 2015. Measurements of carbon-14 with cavity ring-down spectroscopy. Nuclear Instruments and Methods in Physics Research Section B: Beam Interactions with Materials and Atoms 361:277-80.

Minoli G, Prada A, Schuman R, Murnick D, Rigas B. 1998. A simplified urea breath test for the diagnosis of Helicobacter pylori infection using the LARA system. Journal of Clinical Gastroenterology 26(4):264-6.

Murnick D, Dogru O, Ilkmen E. 2010. C-14 analysis via intracavity optogalvanic spectroscopy. Nuclear Instruments & Methods in Physics Research Section B-Beam Interactions with Materials and Atoms 268(7-8):708-11.

Murnick DE, Peer BJ. 1994. Laser-based analysis of carbon-isotope ratios. Science 263(5149):945-7.

Murnick DE, Schuman R, Rigas B. 1995. C-13 Urea breath test with the LARA$^{(TM)}$ system. Gastroenterology 108(4):A172-A.

Murnick DE, Okil JO. 2005. Use of the optogalvanic effect (OGE) for isotope ratio spectrometry of $^{13}CO_2$ and $^{14}CO_2$. Isotopes in Environmental and Health Studies 41(4):363-71.

Murnick DE, Dogru O, Ilkmen E. 2007. Laser based ^{14}C counting, an alternative to AMS in biological studies. Nuclear Instruments and Methods in Physics Research Section B: Beam Interactions with Materials and Atoms 259(1):786-9.

Murnick DE, Dogru O, Ilkmen E. 2008. Intracavity optogalvanic spectroscopy. An analytical technique for C-14 analysis with subattomole sensitivity. Analytical Chemistry 80(13):4820-4.

Okil JO. 2004. Optogalvanic Spectroscopy for Atmospheric Carbon-dioxide Concentration and Isotopic Ratio Measurement [Doctoral Thesis]. Newark: Rutgers, The State University of New Jersey.

Persson A, Eilers G, Ryderfors L, Mukhtar E, Possnert G, Salehpour M. 2013. Evaluation of Intracavity Optogalvanic Spectroscopy for Radiocarbon Measurements. Analytical Chemistry 85(14):6790-8.

Persson A, Berglund M, Salehpour M. 2014a. Improved optogalvanic detection with voltage biased Langmuir probes. Journal of Applied Physics 116(24):243301.

Persson A, Berglund M, Thornell G, Possnert G, Salehpour M. 2014b. Stripline split-ring resonator with integrated optogalvanic sample cell. Laser Physics Letters 11(4):045701.

Persson A, Salehpour M. 2015. Intracavity optogalvanic spectroscopy: Is there any evidence of a radiocarbon signal? Nuclear Instruments and Methods in Physics Research Section B: Beam Interactions with Materials and Atoms Article in Press.

Savarino V, Landi F, Dulbecco P, Ricci C, Tessieri L, Biagini R, Gatta L, Miglioli M, Celle G, Vaira D. 2000. Isotope ratio mass spectrometry (IRMS) versus laser-assisted ratio analyzer (LARA): a comparative study using two doses of. Digestive diseases and sciences 45(11):2168-74.

Spencer LF, Gallimore AD. 2010. Efficiency of CO_2 Dissociation in a Radio-Frequency Discharge. Plasma Chemistry and Plasma Processing 31(1):79-89.

Van der Hulst RWM, Lamouliatte H, Megraud F, Pounder RE, Stoltes M, Vaira D, Williams M, Tytgat GNJ. 1999. Laser assisted ratio analyser C-13-urea breath testing, for the detection of H-pylori: a prospective diagnostic European multicentre study. Alimentary Pharmacology & Therapeutics 13(9):1171-7.

Williams GCR, Smith ALS. 2000. Plasma chemistry of RF discharges in CO_2 laser gas mixtures. Journal of Physics D: Applied Physics 18(3):335-46.